10.48047/jocaaa.2024.33.08.139

MHD Flow and Heat Transfer through circular annulus partially filled with non- Darcy porous medium with moving outer cylinder

[1]Punam Devi, [2*]Dr. Ashok Kumar, [3]Narender Kumar

[1]Research Scholar, Department of Mathematics,
Shri Jagdishprasad Jhabarmal Tibrewala University, Jhunjhunu (Rajasthan), INDIA

[2*]Assistant Professor, Department of Mathematics, GGJ Government College, Hisar (Haryana), INDIA. *Email: sheorangamra@yahoo.co.in*

[3]Assistant Professor, Department of Physics, Dayanand College, Hisar (Haryana), INDIA
*(*Corresponding Author)*

Abstract: In this study, an incompressible fluid flow through circular annulus partially filled with non –Darcy porous medium with moving outer cylinder in the presence of a transverse static magnetic field. The inner region is saturated porous region while annulus is clear fluid region. The governing equations made dimensionless and solved by using Differential Transform Method (DTM). The velocity and temperature for both regions are calculated. The effects of various parameters on velocity and temperature discussed through graphs. The skin-friction coefficient and Nusselt number at the wall of the outer cylinder and at the surface of the concentric inner porous cylinder are discussed.

Keywords: Porous medium, Differential Transform Method, Annulus.

1. INTRODUCTION

The semi-porous medium flow is very useful in industrial area as well as agricultural area. In agriculture, the distribution of pesticides and fertilizers through a cylindrical semi-porous medium is appropriate. The flow through semi porous cylindrical type configurations are encountered in many industries in one or other ways for cooling purposes or for heat connection processes. Hossian M.A. (2013) used integral method to employed the problem of simultaneous heat and mass transfer in two-dimensional free convection from a semi- infinite vertical hot plate. Biazar j.et al.(2010) discussed the differential transform method to employ quadratic Riccati differential equation and results obtained from DTM Method were compared with the results of homotopy analysis method and Adomian decomposition method. Uddin, Z.et al.(2011) analyzed Heat and mass transfer property and the behavior of the flow near the lower stagnation point of a porous isothermal horizontal circular cylinder. Ali, J. (2012) discussed about fifth and sixth order boundary value problems in a finite domain with two-point boundary conditions by using Differential Transform Method. Chamkha, A. (2011) investigated steady, laminar, hyderomagnetic flow, heat and mass transfer through a permeable linearly moving cylinder with heat generation/absorption, chemical reaction, and suction/injection effects in the presence of a uniform transverse magnetic field. Free convection with thermal radiation of a viscous incompressible unsteady MHD flow past a moving vertical cylinder and heat and mass transport in a porous media were discussed by Suneetha, S. et al.'s (2010). Yadav, R.S., et al. (2014) investigated the boundary layer flow and heat transfer of an incompressible, viscous Newtonian fluid along a stretching cylinder in the presence of a constant transverse magnetic field and variable temperature at the surface boundary condition. Nagaraju, G. et al.(2013) described the steady flow of an electrically conducting, incompressible, and micropolar fluid between two concentric rotating vertical cylinders in the presence of an axial magnetic field with a porous lining on the inside of the outer cylinder. Ramachandra Prasad, V. et al. (2013) investigate the steady boundary-layer flow and heat transfer of Casson fluid past a horizontal cylinder under imposed of slip condition in a non-Darcy porous medium. Loganathan et al.(2011) presented effect of magneto dynamics MHD on free convective flow through a moving, semi-infinite vertical cylinder with temperature variation. Kuo, J.S et al.(2013) analyzed the steady Taylor–Couette flow between these two electrically insulated rotating cylinders in the presence of a radial magnetic field and an electrically conducting fluid filled between two concentric cylindrical walls. Gireesha, B.J. et al. (2015) explored the numerical flow of an electrically conducting dusty fluid across an unstable stretched surface in a non-Darcy porous medium utilising the fourth-fifth order Runge-Kutta-Fehlberg scheme, MHD boundary layer flow, and heat transfer. Elbashbeshy and M.A.(2003) investigated the effect of surface mass flux on mixed convection

10.48047/jocaaa.2024.33.08.139

along a vertical plate embedded in porous medium. Yeh,S.et al.(2014) studied the problem of a steady magnetic fluid filled porous annulus between two cylindrical walls in the presence of a Non uniform radially outward magnetic field. Shercliff, J.A. (1953) investigated the steady motion of an electrically conducting, viscous fluid along channels in the influence of an imposed transverse magnetic field under the condition that the walls without currents. The present study focuses on the effect of magnetic field and heat transfer in a moving circular cylinder having a concentric circular porous cylinder of non- Darcy behavior.

2. FORMULATION OF THE PROBLEM

The flow of electrically conducting fluid through a partially filled circular cylinder is considered to be non-Darcy steady, incompressible, and axisymmetric. The porous material cylinder of radius ai and the outer cylinder of radius a (ai<a) is concentric and of velocity v0. In cylindrical coordinates (r,θ, z) the axis of cylinder coincides with the z-axis. On the cylinder, a static magnetic field with the strength (B_0, 0, 0) is applied. Therefore, the flow in the region $0 \leq r \leq ai$ is non-Darcy flow, while in region $ai \leq r \leq a$ is annulus fluid flow.

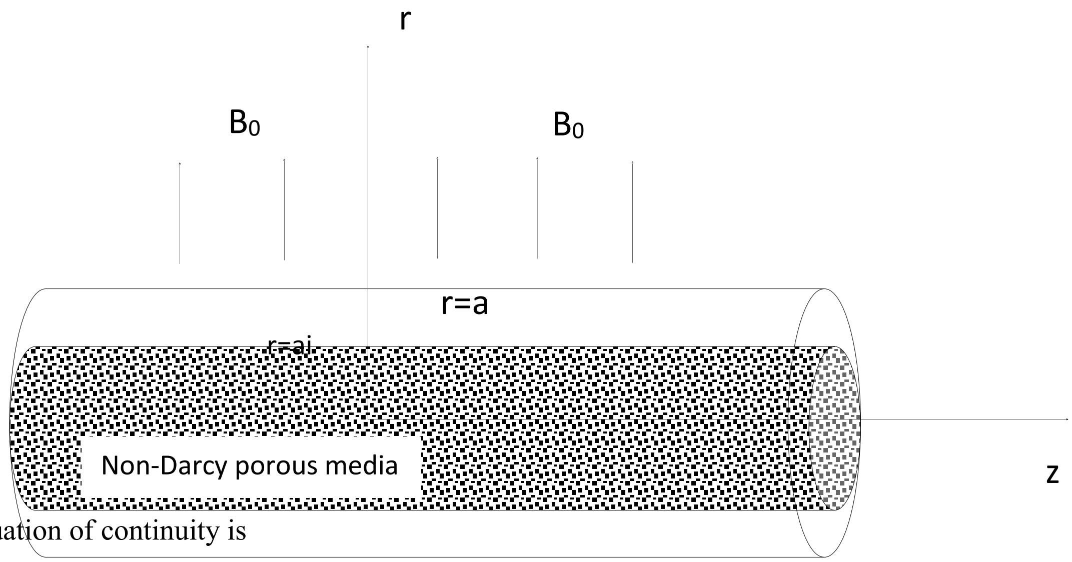

Figure 1: Model of the problem

The equation of continuity is

$$\nabla.\vec{q} = 0 \tag{1}$$

The equations of motion are

$$\rho(\vec{q}.\nabla\vec{q})\vec{q} = -\nabla p + \mu\nabla^2\vec{q} - \frac{\mu}{K}\vec{q} - \frac{\mu c_d}{\sqrt{K\upsilon}}|\vec{q}|\vec{q} + \vec{J}\times\vec{B} \tag{2}$$

The equation of energy

$$\rho c_p(\vec{q}.\nabla\vec{q}) = \nabla^2 T + \frac{\vec{J}^2}{\sigma} \tag{3}$$

The equations of motion and energy for the annular fluid region $ai \leq r \leq a$ are given by under the aforementioned assumptions.

$$\mu\left(\frac{\partial^2 v_{fl}}{\partial r^2} + \frac{1}{r}\frac{\partial v_{fl}}{\partial r}\right) - \frac{\partial p}{\partial x} - \sigma B_0{}^2 v_{fl} = 0 \tag{4}$$

10.48047/jocaaa.2024.33.08.139

$$\kappa\left(\frac{\partial^2 T_{fl}}{\partial r^2}+\frac{1}{r}\frac{\partial T_{fl}}{\partial r}\right)+\sigma B_0^{\,2} v_{fl}^{\,2}=0 \tag{5}$$

The equation of motion and energy for the porous region 0 ≤ r≤ ai are given by

$$\mu\left(\frac{\partial^2 v_{pr}}{\partial r^2}+\frac{1}{r}\frac{\partial v_{pr}}{\partial r}\right)-\frac{\partial p}{\partial x}-\sigma B_0^{\,2} v_{pr}-\frac{\mu}{K}v_{pr}-\frac{\mu}{\sqrt{K}}\frac{c_d}{\upsilon}v_{pr}^{2}=0 \tag{6}$$

$$\kappa\left(\frac{\partial^2 T_{pr}}{\partial r^2}+\frac{1}{r}\frac{\partial T_{pr}}{\partial r}\right)+\sigma B_0^{\,2} v_{pr}^{\,2}=0 \tag{7}$$

The corresponding boundary conditions are

$r=0$: $\quad \frac{\partial v_{pr}}{\partial r}=0, \quad \frac{\partial T_{pr}}{\partial r}=0$ (8)

r=a : $\quad v_{fl}=v_0, \quad T_{fl}=T_w$

r=ai : $\quad v_{fl}=v_{pr} \quad T_{fl}=T_{pr}$ (9)

Where K permeability, v_{fl} and T_{fl} the velocity and temperature of the fluid in the annulus region, v_{pr} and T_{pr} the velocity and temperature of the fluid in the porous region, T_w temperature of the wall of cylinder, T_{pw} temperature at the surface of porous cylinder, ρ the density of the fluid, μ viscosity of the fluid σ electrical conductivity, c_d drag-force constant.

3. METHOD OF SOLUTION

The differential equations (4) to (7) are made dimensionless by the introduction of the following non-dimensional quantities: $r^*=\frac{r}{a}$, $x^*=\frac{x}{a}$, $ai^*=\frac{ai}{a}$, $v_{fl}^{\,*}=\frac{v_{fl}}{V_0}$, $v_{pr}^{\,*}=\frac{v_{pr}}{V_0}$. $G^*=\frac{\partial p}{\partial x}\Big/\frac{\rho V_0^{\,2}}{a}$,

$\mathrm{Re}=\frac{\rho V_0 a}{\mu}$, $M=\sqrt{\frac{\sigma B_0^{\,2}a^2}{\mu}}$,

$Da=\frac{K}{a}$, $F=\frac{c_d\rho V_0^{\,2}a^3}{\sqrt{K}\nu\mu}$, $\theta_{fl}=\frac{T_{fl}-T_w}{T_{pw}-T_w}$, $\theta_p=\frac{T_{pr}-T_w}{T_{pw}-T_w}$, $Br=\frac{\mu V_0^{\,2}}{\kappa\left(T_{pw}-T_w\right)}$

where G the constant dimensionless pressure gradient, Da the Darcy number, Re the Reynolds number, M the Hartmann number, F the Forchheimer number, Br the Brinkman number.

Taking the above substitutions, the non-dimensional equations after dropping asterisks of motion and energy for the clear fluid region and porous region are

$$\frac{d^2 v_{fl}}{dr^2}+\frac{1}{r}\frac{dv_{fl}}{dr}=\mathrm{Re}\,G+M^2 v_{fl} \tag{10}$$

$$\frac{d^2\theta_{fl}}{dr^2}+\frac{1}{r}\frac{d\theta_{fl}}{dr}+M^2 Br\, v_{fl}^{\,2}=0 \tag{11}$$

$$\frac{d^2 v_{pr}}{dr^2}+\frac{1}{r}\frac{dv_{pr}}{dr}=\mathrm{Re}\,G+\left(\frac{1}{Da}+M^2\right)v_{pr}+\frac{F}{\mathrm{Re}}v_{pr}^{\,2} \tag{12}$$

10.48047/jocaaa.2024.33.08.139

$$\frac{d^2\theta_{pr}}{dr^2}+\frac{1}{r}\frac{d\theta_{pr}}{dr}+M^2Br\,{v_{pr}}^2=0 \quad (13)$$

The corresponding boundary conditions are

r = 0: $\frac{\partial v_{pr}}{\partial r}=0$ $\frac{\partial \theta_{pr}}{\partial r}=0$

r=1: $v_{fl}=1$ $\theta_{fl}=0$ (14)

At the interface

r=ai: $v_{fl}=v_{pr}$ $\theta_{fl}=\theta_{pr}$ (15)

By using Differential Transform Method, the solution of momentum and energy equations are obtained.

4. CALCULATION FOR THE VELOCITY PROFILE

4.1Velocity Profile in annulus region

Applying DTM on (10) we will get the following recurrence relation

$$\sum_{i=0}^{h}\delta(i-1)(h-i+1)(h-i+2)V_{fl}\,(h-i+2)+(h+1)V_{fl}(h+1)=GRe\delta(h-1)+M^2\sum_{i=0}^{h}\delta(i-1)\,V_{fl}(h-i) \quad (16)$$

Where $V_{fl}(h)$ is differential transform of $v_{fl}(r)$. Since the value of $v_{fl}(r)$ at r=0 is not known explicitly, therefore assuming $v_{fl}(0)=\alpha$ (constant) which will be determined later with the prescribed boundary conditions.

Put h=0,1,2,3,4,5 in (16), we get

$V_{fl}(1)=0$

$V_{fl}(2)=\frac{1}{4}\left(G\mathrm{Re}+M^2\alpha\right)$

$V_{f}(3)=0$

$V_{fl}(4)=\frac{M^2}{64}(GRe+M^2\alpha)$

$V_{fl}(5)=0$

$V_{fl}(6)=\frac{M^2}{2304}(GRe+M^2\alpha)$

put the above values in the inverse differential transform of $V_f(h)$ the velocity profile is given by

$v_{fl}(r)=\sum_{r=0}^{6}V_{fl}(k)\,r^k$

$v_{fl}(r)=V_{fl}(0)+V_{fl}(1)r+V_{fl}(2)r^2+V_{fl}(3)r^3+V_{fl}(4)r^4+V_{fl}(5)r^5+V_{fl}(6)r^6$

$$v_{fl}(r)=\alpha+\frac{1}{2^2}(GRe+M^2\alpha)r^2+\frac{M^2}{2^24^2}(GRe+M^2\alpha)r^4+\frac{M^4}{2^24^26^2}(GRe+M^2\alpha)r^6 \quad (17)$$

By using the boundary condition at $r=1$, $V_{fl}=1$

$1=\alpha+\frac{1}{2^2}(GRe+M^2\alpha)+\frac{M^2}{2^24^2}(GRe+M^2\alpha)+\frac{M^4}{2^24^26^2}(GRe+M^2\alpha)$

$1=\left(1+\frac{M^2}{4}+\frac{M^4}{64}+\frac{M^6}{2304}\right)\alpha+\left(\frac{1}{4}+\frac{M^2}{64}+\frac{M^4}{2304}\right)GRe$

$\left(1+\frac{M^2}{4}+\frac{M^4}{64}+\frac{M^6}{2304}\right)\alpha=1-\left(\frac{1}{4}+\frac{M^2}{64}+\frac{M^4}{2304}\right)GRe$

the arbitrary constant 'α' is obtained and given by

10.48047/jocaaa.2024.33.08.139

$$\alpha = \frac{1-(\frac{1}{4}+\frac{M^2}{64}+\frac{M^4}{2304})GRe}{(1+\frac{M^2}{4}+\frac{M^4}{64}+\frac{M^6}{2304})}$$

Using value of 'α' in the equation (17), we get the velocity profile of the fluid in the annulus region.

4.2 Velocity profile in porous region

Applying DTM on (11), we get the recurrence relation

$$\sum_{i=0}^{h}\delta(i-1)(h-i+1)(h-i+2)V_{pr}(h-i+2)+(h+1)V_{pr}(h+1)=GRe\delta(h-1)+(\frac{1}{Da}+M^2)\sum_{i=0}^{h}\delta(i-1)\,V_{pr}(h-i)+\frac{F}{Re}\sum_{i=0}^{h}\sum_{s=0}^{i}\delta(s-1)V_{pr}(i-s)V_{pr}(h-i) \qquad (18)$$

Where, the differential transform of $V_{pr}(h)$ is $v_{pr}(r)$. Since value of $v_{pr}(r)$ is not known explicitly at r=0, therefore assuming $V_{pr}(0)=\beta$ (constant), which will be determined later by using interface conditions. Now for h=0, 1, 2, 3, 4, 5 the recurrence relation (18) gives

$$V_{pr}(1)=0$$

$$V_{pr}(2)=\frac{1}{2^2}(GRe+(\frac{1}{Da}+M^2)\beta+\frac{F}{Re}(\beta^2))$$

$$V_{pr}(3)=0$$

$$V_{pr}(4)=\frac{1}{2^2 4^2}\left(\frac{1}{Da}+M^2+2\frac{F}{\text{Re}}\beta\right)\left(\text{Re}G+\left(\frac{1}{Da}+M^2\right)\beta+\frac{F}{\text{Re}}\beta^2\right)$$

$$V_{pr}(5)=0$$

$$V_{pr}(6)=\frac{1}{2^2 4^2 6^2}\left(\frac{1}{Da}+M^2+2\frac{F}{\text{Re}}\beta\right)^2\left(\text{Re}G+\left(\frac{1}{Da}+M^2\right)\beta+\frac{F}{\text{Re}}\beta^2\right)+\frac{1}{4^2 6^2}\left(\text{Re}G+\left(\frac{1}{Da}+M^2\right)\beta+\frac{F}{\text{Re}}\beta^2\right)^2$$

Using these values in the inversion of $V_{pr}(h)$, we have

$$v_{pr}(r)=\sum_{k=0}^{6}V_{pr}(r)\,r^k$$

$$v_{pr}(r)=V_{pr}(0)+V_{pr}(1)r+V_{pr}(2)r^2+V_{pr}(3)r^3+V_{pr}(4)\,r^4+V_{pr}(5)r^5+V_{pr}(6)r^6$$

$$v_{pr}(r)=\beta+\frac{1}{2^2}(\text{ReG}+(\frac{1}{Da}+M^2)\beta+\frac{F}{Re}\beta^2)r^2+\frac{1}{2^2 4^2}(\frac{1}{Da}+M^2+2\frac{F}{Re}\beta)\left(ReG+\left(\frac{1}{Da}+M^2\right)\beta+\frac{F}{Re}\beta^2\right)r^4+\left[\!\left[\frac{1}{2^2 4^2 6^2}\left(\frac{1}{Da}+M^2+2\frac{F}{Re}\beta\right)^2\left(ReG+\left(\frac{1}{Da}+M^2\right)\beta+\frac{F}{Re}\beta^2\right)+\frac{1}{4^2 6^2}(ReG+\left(\frac{1}{Da}+M^2\right)\beta+\frac{F}{Re}\beta^2)^2\right]\!\right]r^6 \qquad (19)$$

Now the interface condition provides that

$$\alpha+\left(\frac{ai^2}{4}+\frac{M^2ai^4}{64}+\frac{M^4ai^6}{2304}\right)(ReG+M^2\alpha)=\beta+\frac{1}{2^2}(\text{ReG}+(\frac{1}{Da}+M^2)\beta+\frac{F}{Re}\beta^2)ai^2+\frac{1}{2^2 4^2}(\frac{1}{Da}+M^2+2\frac{F}{Re}\beta)\left(ReG+\left(\frac{1}{Da}+M^2\right)\beta+\frac{F}{Re}\beta^2\right)ai^4+\left[\!\left[\frac{1}{2^2 4^2 6^2}\left(\frac{1}{Da}+M^2+2\frac{F}{Re}\beta\right)^2\left(ReG+\left(\frac{1}{Da}+M^2\right)\beta+\frac{F}{Re}\beta^2\right)+\frac{1}{4^2 6^2}(ReG+\left(\frac{1}{Da}+M^2\right)\beta+\frac{F}{Re}\beta^2)^2\right]\!\right]ai^6$$

(20)

10.48047/jocaaa.2024.33.08.139

Now (20) is a fourth-degree polynomial in β. A MATLAB code has been generated for the computation of unknown constant β and using this value, the velocity profile in the porous region is known, computed and presented through graphs.

5. CALCULATIONS FOR TEMPERATURE PROFILES

5.1Temperature Profile in Annulus Region

Applying DTM on (12), we get recurrence relation

$$\sum_{i=0}^{h}\delta(i-1)(h-i+1)(h-i+2)\,\phi_{fl}(h-i+2)+(h+1)\phi_{fl}(h+1)=$$
$$-M^2Br\sum_{i=0}^{h}\sum_{s=0}^{i}\delta(s-1)V_{fl}\,(i-s)V_{fl}(h-i) \qquad (21)$$

Where, the differential transform of $\theta_f(r)$ is $\phi_{fl}(h)$ .Let $\theta_{fl}(0)=\gamma$ (constant) will be determined by using boundary condition on $\theta_f(r)$.

Put h=0,1,2,3,4,5,6,7 in equation (21), we get

$\phi_{fl}(1)=0$

$\phi_{fl}(2)=\frac{-M^2Br}{4}\alpha^2$

$\phi_{fl}(3)=0$

$\phi_{fl}(4)=\frac{-M^2Br\alpha}{8}$

$\phi_{fl}(5)=0$

$\phi_{fl}(6)=\frac{-M^2Br}{36}(\,2\alpha V_{fl}(4)+V_{fl}(2)V_{fl}(2))$

$\phi_{fl}(7)=0$

$\phi_{fl}(8)=\frac{-M^2Br}{32}\left(\alpha V_{fl}(6)+V_{fl}(2)V_{fl}(4)\right)$

By using these values in the inversion of differential transform of $\phi_{fl}(h)$

$$\theta_{fl}(r)=\gamma+\phi_{fl}(2)r^2+\phi_{fl}(4)r^4+\phi_{fl}(6)r^6+\phi_{fl}(8)r^8 \qquad (22)$$

By using of boundary condition $\theta_f(1)=0$

$0=\gamma+\phi_{fl}(2)+\phi_{fl}(4)+\phi_{fl}(6)+\phi_{fl}(8)$

the value of γ is determined and given by

$\gamma=\phi_{fl}(2)-\phi_{fl}(4)-\phi_{fl}(6)-\phi_{fl}(8)$

Now, the temperature profile in the annulus region is given by

$\theta_{fl}(r)=\gamma+\phi_{fl}(2)r^2+\phi_{fl}(4)r^4+\phi_{fl}(6)r^6+\phi_{fl}(8)r^8$

$\theta_{fl}(r)=\frac{M^2Br\alpha^2}{4}(1\text{-}r^2)+\frac{M^2Br\alpha}{32}(GRe+M^2\alpha)(1\text{-}r^4)+\frac{M^2Br}{36}(\frac{\alpha M^2}{32}(GRe+M^2\alpha)+\frac{1}{16}(GRe+M^2\alpha))(1\text{-}r^6)+\frac{M^2Br}{32}(\alpha(\frac{M^4}{2304}(GRe+M^2\alpha)+\frac{M^2}{625}(GRe+M^2\alpha))\,(1\text{-}r^8$

5.2 Temperature Profile for Porous Region

Applying DTM on (13), we obtain recurrence relation

$$\sum_{i=0}^{h}\delta(i-1)(h-i+1)(h-i+2)\,\phi_{pr}(h-i+2)+(h+1)\phi_{pr}(h+1)=$$
$$-M^2Br\sum_{i=0}^{h}\sum_{s=0}^{i}\delta(s-1)V_{pr}\,(i-s)V_{pr}(h-i) \qquad (23)$$

10.48047/jocaaa.2024.33.08.139

Where the differential transform of $\theta_{pr}(r)$ is $\phi_{pr}(h)$ .Since the value of $\phi_{pr}(0)$ is not known, therefore its differential transform $\phi_{pr}(0)=b$ (constant) will be determined by using interface condition.

Put h=0,1,2,3,4,5,6,7 in the recurrence relation (23)

$\phi_{pr}(1) = 0$

$\phi_{pr}(2) = \frac{-M^2 Br\beta^2}{4}$

$\phi_{pr}(3) = 0$

$\phi_{pr}(4) = \frac{-M^2 Br\beta V_{pr}(2)}{8}$

$\phi_{pr}(5) = 0$

$\phi_{pr}(6) = \frac{-M^2 Br}{36}(2\,\beta\, V_{pr}(4) + {V_{pr}}^2(2))$

$\phi_{pr}(7) = 0$

$\phi_{pr}(8) = -\frac{M^2 Br}{32}\left(\beta V_{pr}(6) + V_{pr}(2)V_{pr}(4)\right)$

Using these values we get

$$\theta_{pr}(r) = b + \phi_{pr}(2)r^2 + \phi_{pr}(4)r^4 + \phi_{pr}(6)r^6 + \phi_{pr}(8)r^8 \tag{24}$$

On applying the interface condition the equation (28), gives the value of unknown constant b.

$$b = \gamma + \left(\phi_{fl}(2) - \phi_{pr}(2)\right)ai^2 + \left(\phi_{fl}(4) - \phi_{pr}(4)\right)ai^4 + \left(\phi_{fl}(6) - \phi_{pr}(6)\right)ai^6 + \left(\phi_{fl}(8) - \phi_{pr}(8)\right)ai^8 \tag{25}$$

Invoking value of b in (25), the temperature profiles for porous region is computed from (24) with help of MATLAB programming and presented through graphs.

6. SKIN FRICTION COEFFICIENT

The non-dimensional shearing stress at the surface of the porous cylinder and the wall of the circular pipe is calculated as follows in terms of the local skin-friction coefficient and the results are shown in Tables 1 and 2.

$$S_f = \left(\frac{\mu \frac{\partial v}{\partial r}}{\rho {V_0}^2}\right)_{r=ai} \tag{26}$$

The skin friction at the wall of the pipe

$$S_f = \frac{1}{\mathrm{Re}}\left(\frac{\partial v_{fl}}{\partial r}\right)_{r=1} \tag{27}$$

The skin friction at the surface of the porous cylinder

$$S_p = \frac{1}{\mathrm{Re}}\left(\frac{\partial v_{pr}}{\partial r}\right)_{r=ai} \tag{28}$$

10.48047/jocaaa.2024.33.08.139

7. NUSSELT NUMBER

The non-dimensional coefficient of heat transfer at the wall of the circular pipe and at the surface interface of the porous cylinder is obtained as follows and computed values are given in Table 3 and 4.

Nusselt number at the wall of the pipe

$$Nu = -\left(\frac{\partial \theta_{fl}}{\partial r}\right)_{r=1} \quad (29)$$

Nusselt number at the surface of the porous cylinder

$$Nu = -\left(\frac{\partial \theta_{pr}}{\partial r}\right)_{r=ai} \quad (30)$$

8. RESULTS AND DISCUSSION

The effect of magnetic field on fluid flow profile is shown in figure 2.it is demonstrated that the strength of transverse magnetic field is increased the velocity gradient is increased in non- Darcy porous media and decreased in annulus region with the increase of Hartmann number. It is observed in figure 3 that the increase in Reynolds number enhances the fluid velocity in porous region as well as in annulus region. In figure 4 and 5, when F=1, F=5 there is increment in fluid velocity but when F=10 fluid velocity decreased and when F=15 then it is increased and when Da=0.01,Da=0.1 there is small increment in fluid velocity and Da=0.5 ,Da=1 fluid velocity is decreased in annulus region and in annulus region there is small effect of Forchheimer and Darcy number on fluid velocity. Figure 6. depicts that fluid velocity augmented with the decrease of pressure gradient in porous region as well as in annulus region. In figure 7.it is plausible that on increasing magnetic strength i.e. the Hartmann number the fluid temperature significantly increased in porous region and fluid temperature flow is unaffected by the mild transverse magnetic field. Fluid temperature profiles are in parabolic as observed in Figure 8 and 12. Figure 8 and 12 also represented the effect of Reynolds number and Brinkman number on fluid temperature.it is depicted that with the increase of Reynolds number and Brinkman number enhanced the fluid temperature in porous region but there is small effect in annulus region .In figure 9 and 10,fluid temperature decelerate with the increment of Forchheimer number and and Darcy number in porous region and fluid temperature also unaffected in annulus region. The effect of Pressure Gradient on fluid temperature is shown through figure 11, fluid temperature is augmented with the decrement of pressure gradient in porous region and small change in fluid temperature in annulus region. From Table 1 and 2 it is observed that shear stress decreases at the wall of cylinder but increases at the surface of porous cylinder with the increase of Hartmann number and skin friction decreases with the increase of Reynolds number in outer cylinder but increases in porous cylinder. In Table 3 and 4, heat convection increases for small values of Hartmann number up to 3 and then decreases in outer cylinder but in porous cylinder heat convection decreases. Increase in Reynolds number, Brinkman number and Pressure Gradient enhance the heat convection both at annulus wall and porous surface.

9. CONCLUSIONS

- With a rise in Hartmann number, the shear stress at the surface of the core cylinder decreases, and the magnetic field is working as a shear controlling device
- In the porous region, the fluid temperature rises as the Reynolds number and Brinkman number rise, while this effect is small in the annulus region.
- With an increasing Hartmann number, skin friction decreases at the cylinder wall but increases at the porous cylinder's surface.
- With a rise in Brinkman number, Reynolds number, and pressure gradient, the heat convection was improved.
- As the Darcy number at the surface of the porous cylinder increases, the heat convection decreases.

Table 1.Skin Friction at the wall of outer cylinder

10.48047/jocaaa.2024.33.08.139

M	Re	F	Da	G	C_f
1	10	5	0.1	-10	-4.4189
3	10	5	0.1	-10	-5.5762
5	10	5	0.1	-10	-13.474
8	10	5	0.1	-10	-12.7006
5	10	5	0.1	-10	-13.474
5	20	5	0.1	-10	-15.7196
5	30	5	0.1	-10	-16.4682
5	40	5	0.1	-10	-16.8425
5	10	1	0.1	-10	-13.474
5	10	5	0.1	-10	-13.474
5	10	10	0.1	-10	-13.474
5	10	15	0.1	-10	-13.474
5	10	5	0.1	-1	2.6948
5	10	5	0.1	-10	-13.474
5	10	5	0.1	-15	-22.4566
5	10	5	0.1	-20	-31.4393
5	10	5	1	-10	-13.474
5	10	5	0.5	-10	-13.474
5	10	5	0.1	-10	-13.474
5	10	5	0.01	-10	-13.474

Table 2.Skin Friction at the wall of Porous cylinder

M	Re	F	Da	G	C_f
1	10	5	0.1	-10	310.3597
3	10	5	0.1	-10	380.8119
5	10	5	0.1	-10	833.2759
8	10	5	0.1	-10	2646.20
5	10	5	0.1	-10	833.2759
5	20	5	0.1	-10	1296.40
5	30	5	0.1	-10	1522.60
5	40	5	0.1	-10	1655.90
5	10	1	0.1	-10	1647.40
5	10	5	0.1	-10	833.2759
5	10	10	0.1	-10	352.8725
5	10	15	0.1	-10	258.1841
5	10	5	1	-10	472.0509
5	10	5	0.5	-10	488.9932
5	10	5	0.1	-10	833.2759
5	10	5	0.01	-10	7860.20
5	10	5	0.1	-1	750.0281
5	10	5	0.1	-10	833.2759
5	10	5	0.1	-15	875.4565
5	10	5	0.1	-20	917.2307

10.48047/jocaaa.2024.33.08.139

Table 3.Nusselt number at the wall of outer cylinder

M	Re	F	Da	G	Br	Nu
1	10	5	0.1	-10	0.1	8.5192
3	10	5	0.1	-10	0.1	15.115
5	10	5	0.1	-10	0.1	9.7645
8	10	5	0.1	-10	0.1	6.1341
5	10	5	0.1	-10	0.1	9.7645
5	20	5	0.1	-10	0.1	33.1719
5	30	5	0.1	-10	0.1	70.3561
5	40	5	0.1	-10	0.1	121.3173
5	10	1	0.1	-10	0.1	9.7645
5	10	5	0.1	-10	0.1	9.7645
5	10	10	0.1	-10	0.1	9.7645
5	10	15	0.1	-10	0.1	9.7645
5	10	5	0.1	-1	0.1	0.4770
5	10	5	0.1	-10	0.1	9.7645
5	10	5	0.1	-15	0.1	19.746
5	10	5	0.1	-20	0.1	33.1719
5	10	5	1	-10	0.1	9.7645
5	10	5	0.5	-10	0.1	9.7645
5	10	5	0.1	-10	0.1	9.7645
5	10	5	0.01	-10	0.1	9.7645
5	10	5	0.1	-10	0.01	0.9764
5	10	5	0.1	-10	0.05	4.8822
5	10	5	0.1	-10	0.1	9.7645
5	10	5	0.1	-10	0.2	19.5289

Table 4.Nusselt number at the wall of Porous cylinder

M	Re	F	Da	G	Br	Nu
1	10	5	0.1	-10	0.1	-14.5792
3	10	5	0.1	-10	0.1	-52.1656
5	10	5	0.1	-10	0.1	5683.70
8	10	5	0.1	-10	0.1	185020
5	10	5	0.1	-10	0.1	5683.70
5	20	5	0.1	-10	0.1	15596.00
5	30	5	0.1	-10	0.1	21783.0
5	40	5	0.1	-10	0.1	25739.00
5	10	1	0.1	-10	0.1	26294.00
5	10	5	0.1	-10	0.1	5683.70
5	10	10	0.1	-10	0.1	-231.6449
5	10	15	0.1	-10	0.1	-230.2411
5	10	5	0.1	-1	0.1	4239.20
5	10	5	0.1	-10	0.1	5683.70
5	10	5	0.1	-15	0.1	6400.80
5	10	5	0.1	-20	0.1	7128.80
5	10	5	1	-10	0.1	111.7235
5	10	5	0.5	-10	0.1	141.6407
5	10	5	0.1	-10	0.1	5683.70
5	10	5	0.01	-10	0.1	560870
5	10	5	0.1	-10	0.01	568.3709
5	10	5	0.1	-10	0.05	2841.90
5	10	5	0.1	-10	0.1	5683.70
5	10	5	0.1	-10	0.2	11367.00

10.48047/jocaaa.2024.33.08.139

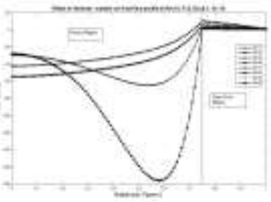

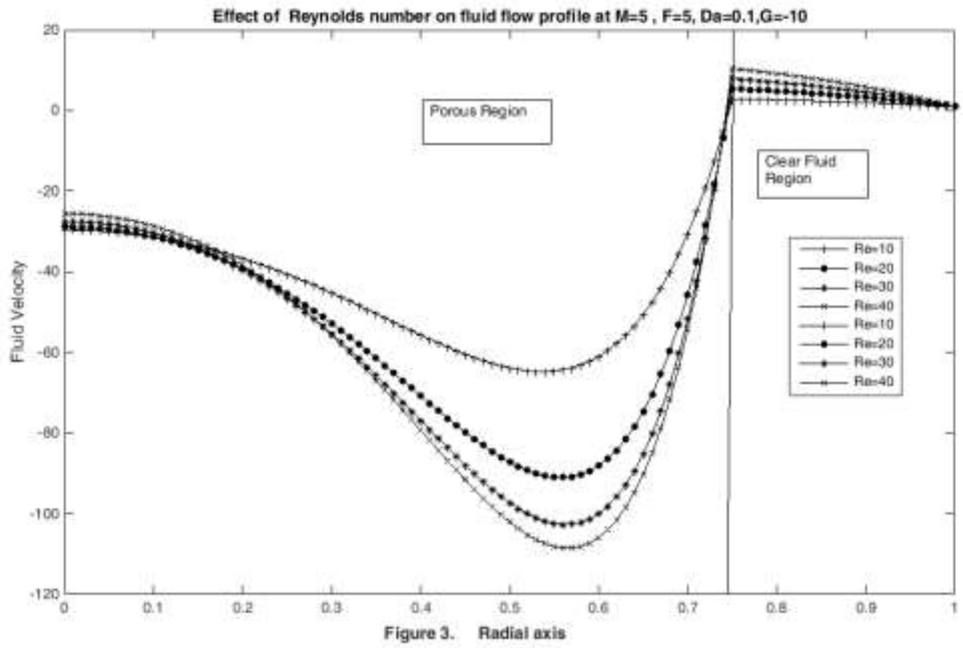

10.48047/jocaaa.2024.33.08.139

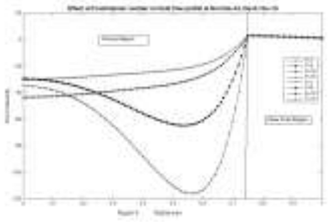

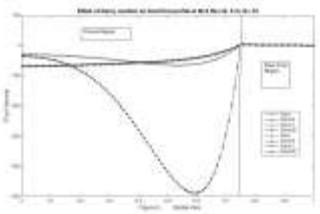

10.48047/jocaaa.2024.33.08.139

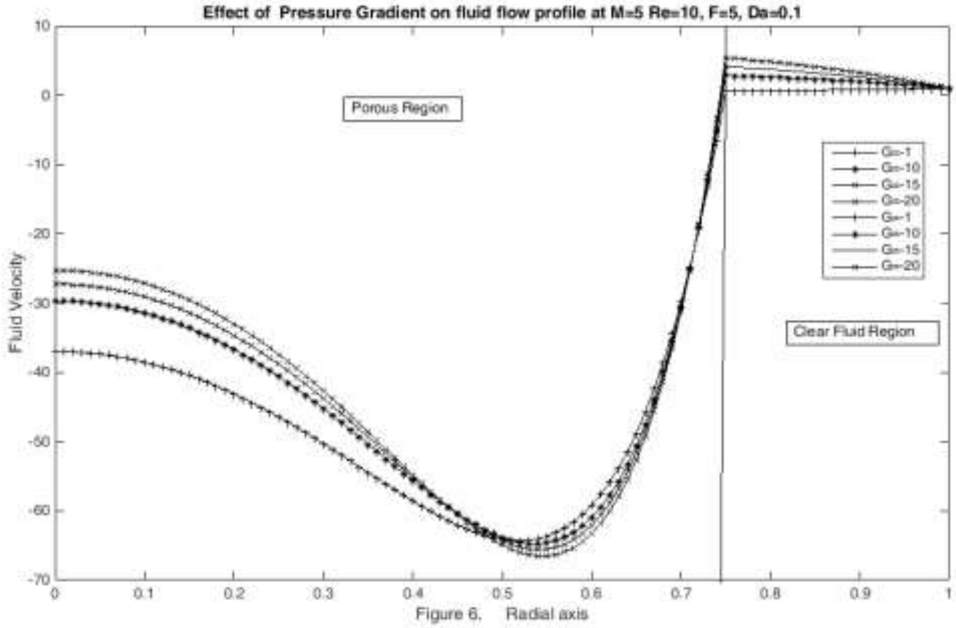

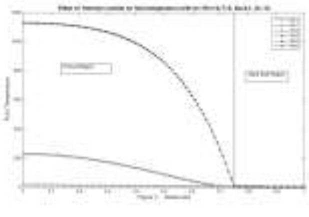

10.48047/jocaaa.2024.33.08.139

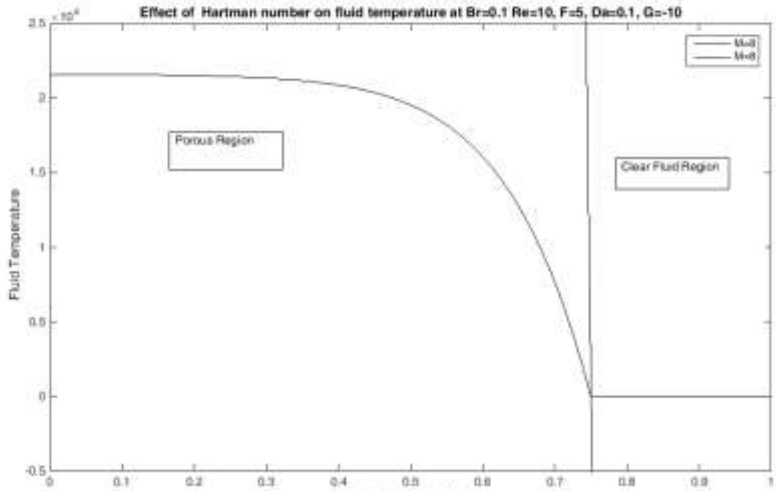

Figure 7.

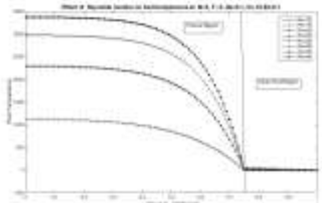

10.48047/jocaaa.2024.33.08.139

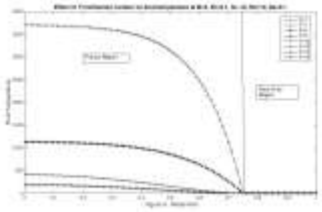

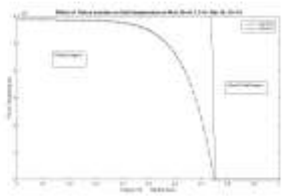

10.48047/jocaaa.2024.33.08.139

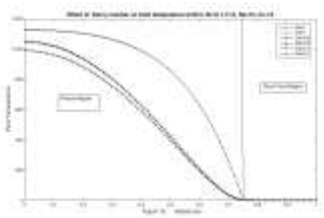

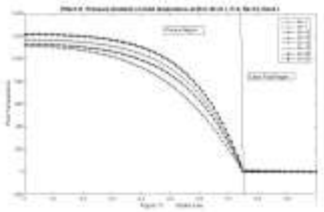

10.48047/jocaaa.2024.33.08.139

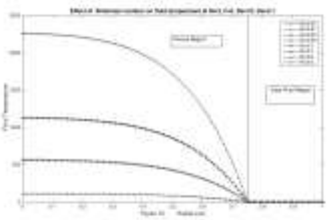

Reference

[1] Hossain, M.A., 1988. Simultaneous heat and mass transfer on oscillatory free convection boundary layer flow. International Journal of Energy Research, 12(2), pp.205-216.

[2] Biazar, J. and Eslami, M., 2010. Differential transform method for quadratic Riccati differential equation. International Journal of Nonlinear Science, 9(4), pp.444-447.

[3] Uddin, Z. and Kumar, M., 2011. MHD Heat and Mass Transfer Free Convection Flow near The Lower Stagnation Point of an Isothermal Cylinder Imbedded in Porous Domain with the Presence of Radiation. *Jordan Journal of Mechanical & Industrial Engineering*, *5*(2)

[4] Ali, J., 2012. One dimensional differential transform method for some higher order boundary value problems in finite domain. *Int. J. Contemp. Math. Sciences*, *7*(6), pp.263-272

[5] Mirzaee, F., 2011. Differential transform method for solving linear and nonlinear systems of ordinary differential equations. *Applied Mathematical Sciences*, *5*(70), pp.3465-3472

[6] Chamkha, A., 2011. Heat and mass transfer from MHD flow over a moving permeable cylinder with heat generation or absorption and chemical reaction.

[7] Suneetha, S. and Reddy, N.B., 2010. Radiation and mass transfer effects on MHD free convection flow past a moving vertical cylinder in a porous medium. *Journal of Naval Architecture and Marine Engineering*, *7*(1), pp.1-10.

[8] Yadav, R.S. and Sharma, P.R., 2014. Effects of porous medium on MHD fluid flow along a stretching cylinder. *Annals of Pure and Applied Mathematics*, *6*(1), pp.104-113

[9] Nagaraju, G., Murthy, J.R. and Sai, K.S., 2013. STEADY MHD FLOW OF MICROPOLAR FLUID BETWEEN TWO ROTATING CYLINDERS WITH POROUS LINING. *Acta Technica Corviniensis-Bulletin of Engineering*, *6*(3), p.115

[10] Ramachandra Prasad, V., Subba Rao, A. and Anwar Bég, O., 2013. Flow and heat transfer of casson fluid from a horizontal circular cylinder with partial slip in non-darcy porous medium. *J Appl Computational Math*, *2*(127), p.2.

[11] Loganathan, P., Kannan, M. and Ganesan, P., 2011. MHD effects on free convective flow over moving semi-infinite vertical cylinder with temperature oscillation. *Applied Mathematics and Mechanics*, *32*(11), pp.1367-1376

[12] Kuo, J.S. and Leong, J.C., 2013. Analysis of a conducting fluid in a thin annulus with rotating insulated walls under radial magnetic effect. *Applied Mathematical Modelling*, *37*(5), pp.3021-3035.

10.48047/jocaaa.2024.33.08.139

[13] Gireesha, B.J., Mahanthesh, B., Manjunatha, P.T. and Gorla, R.S.R., 2015. Numerical solution for hydromagnetic boundary layer flow and heat transfer past a stretching surface embedded in non-Darcy porous medium with fluid-particle suspension. *Journal of the Nigerian Mathematical Society*, *34*(3), pp.267-285.

[14] Elbashbeshy, E.M.A., 2003. The mixed convection along a vertical plate embedded in non-Darcian porous medium with suction and injection. *Applied Mathematics and Computation*, *136*(1), pp.139-149.

[15] Yeh, S., Chen, T.J. and Leong, J.C., 2014. Analytical solution for MHD flow of a magnetic fluid within a thick porous annulus. *Journal of Applied Mathematics*, *2014*.

[16] Shercliff, J.A., 1953, January. Steady motion of conducting fluids in pipes under transverse magnetic fields. In *Mathematical Proceedings of the Cambridge Philosophical Society* (Vol. 49, No. 1, pp. 136-144). Cambridge University Press.